CHAPTER 4

EQUIVALENT CIRCUIT ANALYSIS OF THE DISC-LOADED COAXIAL STRUCTURE FOR MILO

4.1 Introduction

4.2 Electromagnetic Analysis

4.2.1 *Structure model*
4.2.2 *Electromagnetic field expressions*
4.2.3 *Electromagnetic boundary conditions*
4.2.4 *Equivalent shunt capacitance per unit length*
4.2.5 *Equivalent series inductance per unit length*
4.2.6 *Phase velocity of the structure*
4.2.7 *Dispersion relation*
4.2.8 *Characteristic impedance*

4.3 Results and discussion

4.3.1 *Effect of structure parameters on propagation characteristics*
4.3.2 *Effect of structure parameters on dispersion characteristics*

4.4 Conclusions

4.1 Introduction

To tailor the propagation behavior of the waveguide, it is often loaded with the periodic vanes or discs. An axially periodic disc loaded cylindrical waveguide is frequently being used as slow and as fast-wave transmission line. A metal disc-loaded cylindrical waveguide is considered as periodic electromagnetic (EM) structure. These waveguides finds applications in the passive devices such as filter, antenna, antenna feed, mode converter and in the active devices such as RF interaction structures. These waveguides are also a key component in the slow-wave devices e.g. accelerator, traveling wave tube, backward wave amplifier, MILO, etc. and in the fast-wave devices, e.g., gyro-traveling wave tube, gyro-klystron [Dwivedi *et al.* (2012)]. Disc-loaded cylindrical waveguide is a metallic structure which can capable to bear high power and hence used in the high power devices and systems. Magnetically insulated line oscillator (MILO) which is a gigawatt level of high power microwave (HPM) oscillator, is basically a slow-wave crossed field device operating in the TM_{01} mode. In MILO, disc-loaded waveguide is used as its RF interaction structure with an additional coaxial metallic cylinder at its center [Kesari *et al.* (2010)]. Electromagnetic analysis of the disc loaded waveguide structure has been reported by various authors. Kesari *et al.* have analyzed the metal disc loaded cylindrical structure operating in the *TE* mode using field modal matching technique at the cylindrical interface between disc free and disc occupied regions for its application in the fast-wave regime. Kesari has further extended the analysis for the disc-loaded-coaxial waveguide. Dwivedi and Jain performed the EM analysis of the coaxial disc loaded structure using modal matching field analytical technique for the *TM* modes operating in the slow-wave regime for its application in MILO [Dwivedi

and Jain (2012)]. Qing and Long analyzed the disc loaded slow-wave structure using variational technique and compared their results with those obtained by the field matching method [Jian-Qing *et al.* (2004)]. Minami *et al.* reported dispersion characteristic of lower TM_{0n} mode in a sinusoidal rippled waveguide using linear perturbation theory [Minami, Carmel *et al.* (2005)]. Wang *et al.* analyzed the coaxial disk-loaded structure for the lowest symmetric mode using field matching [Wang *et al.* (2007)].

The equivalent circuit analytical approach is an alternative technique for analyzing the EM structure which is relatively less involved and cumbersome compared to the field analytical approach. In this approach, the actual structure is treated as a transmission line characterized by a set of four distributed line parameters. The propagation characteristics of the structure can be expressed in terms of these line parameters. These line prameters are then resolved by expressing these parameters in terms of the structure dimension. Fan *et al.* analyzed a coaxial periodic disc loaded structure operating in the TM_{01} mode where the structure region between consecutive discs has been considered as a cavity [Wang *et al.* (2007)]. This cavity is modeled using equivalent circuit approach in terms of the series inductance and shunt capacitance per unit length of the equivalent line.

Present chapter deals with analytical study of a metal disc loaded coaxial structure by using equivalent circuit approach, which considered the space harmonics of propagating waves generated due to the axial periodicity of the structure in the disc free region. This approach also takes into account the modal harmonics of stationary waves, supported in the disc occupied region between two consecutive metal discs [Dwivedi and Jain (2012)]. Considering current and voltage Telegraphist's equations, the transmission line parameters such as shunt capacitance per unit length, series

inductance per unit length, phase velocity and the characteristics impedance are analyzed for the proposed structure. In the equivalent circuit approach [Basu (1996)], one has to deal with only half of the total number of boundary conditions at a time. One half set estimates capacitance per unit length while other half estimates inductance per unit length. Further, in this approach, unlike in the field analysis, it is not required to simplify a complex dispersion relation which involves a $n \times m$ determinant. Thus, the equivalent circuit analysis makes the study of loaded structures simpler [Dwivedi and Jain (2012)]. This technique yields same dispersion relation as resulted from the field matching technique. In section II, electromagnetic analysis of the structure is described using Telegraphic equations for the proposed structure. In section III, effect of various structure parameters on various line parameters and variation of phase velocity with frequency is discussed.

4.2 Electromagnetic (EM) Analysis

A disc-loaded coaxial waveguide, where the axial periodic metal discs of finite thickness are projecting radially inward from the metal envelope, is used as the RF interaction in MILO device and also considered for electromagnetic (EM) analysis (Figure 1). The analysis is carried out in the slow-wave operating regime for the symmetrical TM_{0n} operating modes. As discussed in previous sections, the field analysis yields accurate results however it is rather less involved and cumbersome [Dwivedi and Jain (2012)]. In order to simplify the analysis without compromising its accuracy, an equivalent circuit approach is applied. With this approach, the waveguide structure is treated as an equivalent transmission line which is characterized by a set of four distributed line parameters, equivalent series resistance; inductance per unit length; equivalent shunt conductance and capacitance per unit

length. In case of the metal structure, for the sake of the simplicity, lossless condition is considered which enabled the equivalent series resistance and shunt conductance per unit length of the structure as zero. Only two equivalent line parameters, the shunt capacitance per unit length (C_e) and series inductance per unit length (L_e) are considered for the analysis. These line parameters are evaluated with the help of loss-free field expressions and boundary conditions of the structure. Here, one has to deal with only half of the total number of structure boundary conditions and field equations at a time. Thereby makes the equivalent circuit analysis approach simpler though it yields the same results [Kartikeyan *et al*. (1992)].

4.2.1 Structure model

The structure (Figure 1) considered, in our analysis, is consists of a central cylindrical metallic structure of radius (r_c) surrounded by a coaxial cylindrical waveguide (inner wall radius, r_w) with axial periodic metal discs of hole radius r_d projecting radially inward of wall thickness *T* and periodicity *L*. For the EM analysis, the waveguide structure (Figure 1) is divided into the two free-space regions : the disc-free region, labeled as region I; and the disc-occupied region, labeled as region II. The region I occupies the space $r_c \le r \le r_d$, $0 \le z \le \infty$ while region II occupies $r_d \le r \le r_w, 0 \le z \le (L-T)$.

In our analysis, it was assumed that traveling waves are present in the disc-free region (region I), between the central conductor and metal discs. Only standing waves exist in the disc- occupied region (region II), considered between two consecutive discs of the structure.

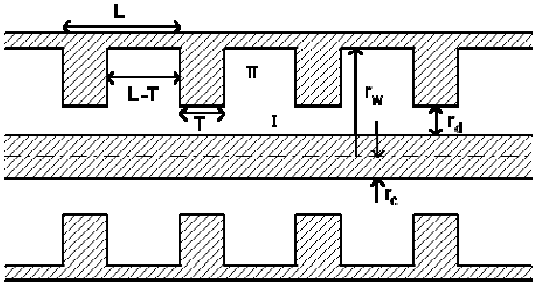

Figure 4.1: Schematic of a disc loaded coaxial cylindrical waveguide structure.

Hence, space harmonics of the traveling-wave are generated due to the axial periodicity of the structure. Modal harmonics of the standing wave caused due to the reflections of the EM waves from the metal discs. The EM field expressions are developed for the regions I and II, which are subsequently used along with the boundary conditions at the interface between the two regions. These expressions are used to obtain the shunt capacitance per unit length (C_e) and series inductance per unit length (L_e). These equivalent circuit line parameters are handy to evaluate the phase velocity, dispersion relation and the characteristic impedance of the structure.

4.2.2 Electromagnetic field expressions

In the cylindrical coordinate system (r, θ, z) one may write the relevant electric and magnetic field expressions [Dwivedi and Jain (2012)] for the azimuthally symmetric *TM* mode ($H_z = 0$) for the region I of the structure (Figure 1):

$$E_z^I = \sum_{n=-\infty}^{\infty} [A_n^I J_0\{\gamma_n^I r\} + B_n^I Y_0\{\gamma_n^I r\}] \exp j(\omega t - \beta_n^I z), \tag{4.1}$$

$$E_r^I = \sum_{n=-\infty}^{\infty} \frac{j\beta_n^I}{\gamma_n^I} [A_n^I J_1\{\gamma_n^I r\} + B_n^I Y_1\{\gamma_n^I r\}] \exp j(\omega t - \beta_n^I z), \tag{4.2}$$

$$H_\theta^I = j\omega\varepsilon \sum_{n=-\infty}^{\infty} \frac{1}{\gamma_n^I}[A_n^I J_1\{\gamma_n^I r\} + B_n^I Y_1\{\gamma_n^I r\}]\exp j(\omega t - \beta_n^I z)\,. \tag{4.3}$$

Superscript 'I' refers the corresponding quantities in disc free region i.e. region I of the structure where traveling wave exist. System periodicities allow utilizing Floquet's theorem, enabling us to write axial propagation constant $\beta_n^I = \beta_0^I \pm 2n\pi / L$. Here, γ_n^I $(= (k^2 - \beta_n^{I^2})^{1/2})$ is the radial propagation constant and k $(= \omega(\mu_0\varepsilon_0)^{1/2})$ is the free space propagation constant. n (= 0, ±1, ±2, ±3, …) represents space harmonic number of the travelling wave present in structure region I. Hence β_n^I is simply written as β_n which is the structure propagation constant. J_0 and J_1 are the Bessel functions of first kind of zeroth and first order, respectively, of the argument $\{\gamma r\}$. Considering the traveling and standing waves in disc-free and disc-occupied regions of structure, respectively, the field expressions for axial electric and azimuthal magnetic field intensities in region II are written using the solution of the wave equation. The stationary wave between the discs consists of forward and backward wave components, latter caused by the reflection from the metal disc surface. Expression [Dwivedi and Jain (2012)] for axial component of electric field intensity, for region II, may be written as follows while considering the boundary condition for the axial electric field at the waveguide's wall which vanishes at $r = r_c$:

$$E_z^{II} = \sum_{m=1}^{\infty} A_m^{II}\,[X_0\{\gamma_m^{II} r\}\exp(j\omega t)\sin(\beta_m^{II} z)]\,, \tag{4.4}$$

$$E_r^{II} = \sum_{m=1}^{\infty} \frac{j\beta_m^{II}}{\gamma_m^{II}} A_m^{II} X_0'\{\gamma_m^{II} r\}\exp(j\omega t)\sin(\beta_m^{II} z) \tag{4.5}$$

where X_0 and its derivative X'_0 are defined as:

$$X_0\{\gamma_m^{II} r\} = Y_0\{\gamma_m^{II} r_w\}J_0\{\gamma_m^{II} r\} - J_0\{\gamma_m^{II} r_w\}Y_0\{\gamma_m^{II} r\}\,, \tag{4.6}$$

$$X_0'\{\gamma_m^{II} r\} = Y_0\{\gamma_m^{II} r_w\} J_1\{\gamma_m^{II} r\} - J_0\{\gamma_m^{II} r_w\} Y_1\{\gamma_m^{II} r\} \tag{4.7}$$

Here, $\gamma_m^{II} = (k^2 - (\beta_m^{II})^2)^{1/2}$ is the radial propagation constant in region II where standing wave is present and gives rise to the modal harmonics m (= 1, 2, 3, ...). $\beta_m^{II}(=m\pi/(L-T))$ which is the axial propagation constant in the disc-occupied region II.

4.2.3 Electromagnetic boundary conditions

The EM boundary conditions are described to predict the structural characteristics. These boundary conditions are pertaining with either the axial or azimuthally components of the electric and magnetic field intensities at the interface between the two regions. The relevant boundary conditions referring to the continuity of the axial electric field intensity and azimuthal component of magnetic field intensity at interface between region I and region II:

$$\left.\begin{aligned} E_z^I &= E_z^{II} \\ H_\theta^I &= H_\theta^{II} \end{aligned}\right\} \text{ at } r = r_d;\ \ 0 < z < (L-T)\ . \tag{4.8}$$

Condition for the axial electric field intensity, at metallic interface, of discontinuity:

$$E_z^I = 0, \quad 0 < z < \infty. \tag{4.9}$$

The discontinuity of the tangential (azimuthal) component of magnetic field intensities at the interface is equal to the surface current density:

$$H_\theta^{II} - H_\theta^I = J_z \ \text{ at } r = r_d;\ \ 0 \le z < (L-T)\,. \tag{4.10}$$

The normal components of electric field intensity are discontinuous at the interface and the amount of discontinuity being equal to the surface charge density ρ_s:

$$E_r^{II} - E_r^I = \frac{\rho_s}{\varepsilon} \quad \text{at } r = r_d; \quad 0 \le z < (L-T), \tag{4.11}$$

assuming $\varepsilon_r^{II} = \varepsilon_r^I = \varepsilon$ at the interface.

4.2.4 Equivalent shunt capacitance per unit length

The equivalent shunt capacitance per unit length for the structure can be obtained using the 'current' Telegraphist's equation of the equivalent transmission line, in order to relate circuit potential with the axial current of the disc-loaded structure [Kartikeyan *et al*. (1992)]:

$$\frac{\partial I_z}{\partial z} + C_e \frac{\partial V}{\partial t} = 0 . \tag{4.12}$$

Considering RF waves to vary as, $\exp j(\omega t - \beta z)$ then above equation can be rewritten as:

$$C_e = \frac{\beta_n}{\omega} \frac{I_z}{V} . \tag{4.13}$$

J_z represent the axial surface current density and taken as:

$$J_z = I_z / 2\pi r_d \quad .$$

Field expressions from equations (4.1) and (4.4) are substituted in the first boundary condition of equation (4.9) to obtain relation between various field constants A_n^I in region I and A_m^{II} in region II, as:

$$\sum_{n=-\infty}^{\infty} [V_0\{\gamma_n^I r\}] \exp j(\omega t - \beta_n^I z) = \sum_{m=1}^{\infty} A_m^{II} X_0\{\gamma_m^{II} r\} \exp(j\omega t) \sin(\beta_m^{II} z) \tag{4.14}$$

where, $$V_0\{\gamma_n^I r\} = A_n^I J_0\{\gamma_n^I r\} + B_n^I Y_0\{\gamma_n^I r\} .$$

Now, the relation between field constants B_n^I and A_n^I is obtained using boundary condition given by (4.10) and resulting expression is substituted in (4.15) which was further multiplied both sides by $\sin(\beta_m^{II} z)$. Further by integrating within limit

$0 \le z < (L-T)$ using orthogonal property of the trigonometric function results in [Dwivedi and Jain (2012)]:

$$A_m^{II} = \sum_{n=-\infty}^{\infty} U_{n,m} A_n^{I} \ . \tag{4.15}$$

where,
$$U_{n,m} = \left(\frac{2\beta_m^{II}}{L-T}\right)\left(\frac{(-1)^m \exp(j\beta_n^{I}(L-T))-1}{\beta_m^{II^2} - \beta_n^{I^2}}\right)\left(\frac{X_0\{\gamma_m^{II} r\}}{Z_0\{\gamma_n^{I} r\}}\right), \tag{4.16}$$

$$Z_0\{\gamma_n^I r\} = Y_0\{\gamma_n^I r_c\} J_0\{\gamma_n^I r\} - J_0\{\gamma_n^I r_c\} Y_0\{\gamma_n^I r\}. \tag{4.17}$$

Further, using boundary condition (4.11) to express field constant A_n^I in terms of circuit current by multiplying both sides by $\sin(\beta_m^{II} z)$ and integrating between the limit $0 \le z < (L-T)$ we get following:

$$\int_0^{(L-T)} (H_\theta^{II} - H_\theta^{I}) \sin(\beta_m^{II} z)\, dz = \int_0^{(L-T)} \frac{I_z}{2\pi r_d} \sin(\beta_m^{II} z)\, dz. \tag{4.18}.$$

In order to express, the field constant A_n^I, in terms of circuit current, the field expressions (4.3) and (4.6) substitutes in (4.19). By substituting expression (4.16) for field constant A_m^{II} in equation (4.19) and after rearranging, it can be written as follows:

$$A_n^I = R_{nm}\{\gamma_n^I r\} I_z \,, \tag{4.19}$$

$$R_{nm}\{\gamma_n^I r\} = \frac{\gamma_n^I \gamma_m^{II} Y_0\{\gamma_n^I r_c\} Z_0\{\gamma_n^I r\} \cos(\beta_m^{II}(L-T)) \exp(-j\omega t)}{2j\omega\varepsilon\pi r_d [\beta_m^{II} X_0\{\gamma_m^{II} r_d)\, X_0'\{\gamma_m^{II} r_d\} Y_0\{\gamma_n^I r_c\} - \gamma_m^{II} J_1\{\gamma_n^I r_d\} Z_0\{\gamma_n^I r\}] S}$$

The axial electric field intensity at the tip of the metal disc ($r = r_d$) can be expressed in terms of the axial current. Substituting equation (4.20) in (4.1) and rearranging (4.1) following expression achieved:

$$E_z^I = \sum_{n=-\infty}^{\infty} A_n^I (Z_0\{\gamma_n^I r_d\} / \mathrm{Y}_0\{\gamma_n^I \mathrm{r}_c\}) \exp j(\omega t) \tag{4.20}$$

$$E_z^I = \sum_{n=-\infty}^{\infty} P_{nm} I_z \,. \tag{4.21}$$

Where, $$P_{nm} = \sum_{n=-\infty}^{\infty} R_{nm}\{\gamma_n^I r\} Z_0\{\gamma_n^I r_d\}. \quad (4.22)$$

Now, the axial electric field intensity [Basu (1996)] can be related to the scalar and vector circuit potential as:

$$E_z = -\frac{\partial V}{\partial z} - \frac{\partial A_z}{\partial t}.$$

Considering RF waves to vary as $\exp j(\omega t - \beta_n z)$, then above equation can be recast:

$$E_z = j\beta_n V - j\omega A_z. \quad (4.23)$$

In the cylindrical coordinate system, vector potential V can be related to the scalar potential A_z

$$\frac{\partial A_z}{\partial z} + \mu\varepsilon \frac{\partial V}{\partial t} = 0 \quad . \quad (4.24)$$

Again considering variation of the RF quantities, Equation (4.25) becomes:

$$-j\beta A_z + j\omega\mu\varepsilon V = 0. \quad (4.25)$$

Substituting the value of scalar potential from (4.26) in (4.24) to get [Basu (1996)]:

$$E_z^I = j\left(\frac{\gamma_n^{I^2}}{\beta_n^I}\right) V \quad . \quad (4.26)$$

The ratio of current to voltage can find by equalizing Equations (4.21) and (4.27) which was further substituted in (4.14) to obtain an expression for the shunt capacitance per unit length in terms of structure parameters as:

$$C_e = \frac{j(\gamma_n^I)^2}{\omega} \frac{1}{P_{nm}}. \quad (4.27)$$

4.2.5 Equivalent series inductance per unit length

Series inductance per unit length of the equivalent transmission line for the

structure under consideration can be obtained using the 'voltage' *Telegraphist's* equation in order to relate the circuit potential with the circuit current as [Basu (1996)]:

$$\frac{\partial V}{\partial z} = -L_e \frac{\partial I_\theta}{\partial t}$$

$$\Rightarrow \qquad L_e = (\frac{\beta_n}{\omega})\frac{V}{I_\theta}. \tag{4.28}$$

To find the ratio of circuit potential and circuit current, V/I_θ, the relation between the field constants, A_n^I for region I and A_m^{II} for region II is required. For this purpose, the field expressions (4.2) and (4.5) are inserted into the second boundary condition of (4.9). Then, the relation between the field constants B_n^I and A_n^I is obtained using (4.10) and resulting expression is substituted in Equation (4.29). This equation is then multiplied both sides by factor $\sin(\beta_m^{II} z)$ and integrating further within the limit $0 \le z < (L-T)$. While using orthogonal property of trigonometric function results in following expression [Dwivedi and Jain (2012)]:

$$A_m^{II} = \sum_{n=-\infty}^{\infty} X_{n,m}\, A_n^I \ , \tag{4.29}$$

where,

$$X_{n,m} = \left(\frac{2\beta_m^{II}}{L-T} \times \frac{(-1)^m \exp(\mathrm{j}\beta_n^I(\mathrm{L}-\mathrm{T})) - 1}{\beta_m^{II^2} - \beta_n^{I^2}}\right)\left(\frac{Z_0'\{\gamma_n^I r\}}{X_0'\{\gamma_m^{II} r\} Y_0\{\gamma_n^I r_c\}}\right)\frac{\gamma_m^{II}}{\gamma_n^I} \tag{4.30}$$

Boundary conditions, given in Equation (4.12), are used to express field constant, A_n^I, in terms of circuit current. Further, rearranging Equation (4.12), an azimuthal sheet current I_θ arises due to the discontinuity in unit time. $E_r^{II} - E_r^I = \frac{\rho_s}{\varepsilon} = \frac{1}{\varepsilon}\left(\frac{q}{A}\right) = \frac{I_\theta}{2\pi r_d \varepsilon}$,

where the surface charge density ρ_s can be written as the ratio of total surface charge q to area A. Multiplying both sides by factor $\sin(\beta_m^{II} z)$ and integrated between the limit $0 \le z < (L-T)$,

$$\int_0^{(L-T)} (E_r^{II} - E_r^{I}) \sin(\beta_m^{II} z)\, dz = \int_0^{(L-T)} \frac{I_\theta}{(2\pi r_d)\varepsilon} \sin(\beta_m^{II} z)\, dz \,. \tag{4.31}$$

Substituting field expressions (4.2) and (4.5) in (4.32) and value of field constant from (4.30) in the above equation to obtain:

$$A_n^I = \sum_{n=-\infty}^{\infty} Q_{nm} I_\theta \,, \tag{4.32}$$

$$Q_{nm} = \frac{\gamma_n^I \gamma_m^{II} Y_0\{\gamma_n^I r_c\} \cos(\beta_m^{II}(L-T))}{j2\pi\varepsilon \mathrm{r}_d [\beta_m^{II} \gamma_n^I Z_0'\{\gamma_n^I r_d\} - \beta_n^I \gamma_m^{II} Z_0'\{\gamma_n^I r\}] S \exp(-j\omega t)} \,. \tag{4.33}$$

By substituting field constant value, obtained from (4.33), into (4.21) to express the axial electric field intensity in terms of circuit current as:

$$E_z^I = W_{nm} I_\theta \,, \tag{4.34}$$

Where, $W_{nm} = Q_{nm} Z_0\{\gamma_n^I r_d\}$.

Now, substituting expression for Q_{nm} from (4.34) in above:

$$W_{nm} = \frac{\gamma_n^I \gamma_m^{II} Z_0\{\gamma_n^I r_d\} \cos(\beta_m^{II}(L-T))}{j2\pi\omega\varepsilon r_d [\beta_m^{II} \gamma_n^I Z_0'\{\gamma_n^I r_d\} - \beta_n^I \gamma_m^{II} Z_0'\{\gamma_n^I r\}] \mathrm{S}} \,. \tag{4.35}$$

Equating equations (4.27) and (4.35) to find the ratio of circuit potential and circuit current, V/I_θ, then substituted resulting expression in (4.29) to find the equivalent series inductance per unit length in terms of structure parameters as:

$$L_e = \frac{1}{j\omega} \left(\frac{\beta_n}{\gamma_n^I} \right)^2 W_{nm} \,. \tag{4.36}$$

4.2.6 Phase velocity of the structure

As we know that the phase velocity along the waveguide for all the normal modes is greater than the speed of light; this property presents a limitation as it does not allow interactions with the slow space charge waves present with the electron beam of the slow-wave microwave devices like MILO. The solution to this limitation is to introduce a periodic variation in some property of waveguide in order to reduce the phase velocities below the speed of light in the direction of propagation of the electron beam. This might involve axial or azimuthal periodic loading of the waveguide forming resonant cavities. Considering the analysis described in preceding sections, the shunt capacitance and series inductance per unit length of the equivalent transmission line of the coaxial disc loaded structure are obtained. Then these line parameters can readily be used to calculate the phase velocity of the structure. This is an important propagation parameter for the analysis and design of the slow-wave RF interaction structure. The phase velocity v_p of coaxial disc loaded structure can be calculated using the well known relationship:

$$v_p = 1/(L_e C_e)^{1/2}. \tag{4.37}$$

Substituting the expressions of the equivalent shunt capacitance Equation (4.28) and series inductance per unit length Equation (4.37) in (4.38) the phase velocity can be obtained. Equations obtained represent a set of homogeneous linear equations. The vanishing determinant of these Equations, as a condition of the non-trivial solution, gives the dispersion relation of the structure.

4.2.7 Dispersion relation

Dispersion relation is used to characterize the EM wave propagation behavior of the waveguide. We have developed expressions in the preceding sections for the

series inductance per unit length and the shunt capacitance per unit length of the equivalent line can be used to obtain the dispersion relation of the structure as:

$$\beta^2 - \omega^2 L_e C_e = 0 .$$

Using Equations (4.28) and (4.37) in above equation leads to dispersion relation in terms of structure parameters and is same as derived by field analysis [Dwivedi *et al*. (2012)]. Above equation can also be written as:

$$\sum_{n=-\infty}^{\infty} (M_{n,m} - N_{n,m}) = 0 \quad (m = 1, 2, 3, ...) \quad . \tag{4.38}$$

The above dispersion relation (4.39) is same as derived using a more involved and field analysis approach [Dwivedi *et al*. (2012)], where

$$M_{n,m} = \left(\frac{X_0\{\gamma_m^{II} r\}}{Z_0\{\gamma_n^{I} r\}} \right) S \quad ,$$

and

$$N_{n,m} = \left(\frac{\gamma_m^{II}}{\gamma_n^{I}} \right) \left(\frac{Z_0'\{\gamma_n^{I} r\}}{Y_0\{\gamma_n^{I} r_c\} X_0'\{\gamma_m^{II} r\}} \right) S \quad .$$

The dispersion relation of the structure is obtained here by applying the equivalent circuit approach and used to plot the dispersion characteristics as well as study the role of structure parameters to control its shape.

4.2.8 Characteristic impedance

The characteristic impedance of line is another important parameter from the circuit matching considerations. It can be easily calculated using the known relation as:

$$Z_0 = (L_e / C_e)^{1/2} . \tag{4.39}$$

4.2.9 Special cases

As special case the simple dispersion relation (4.39) for the disc loaded coaxial waveguide structure, using an equivalent circuit approach, passes on to the more involved dispersion relations of the other type of cylindrical RF structures which obtained through modal matching field analytical approach. For a disc loaded cylindrical waveguide structure, on substituting cathode radius as zero ($r_c = 0$) in expression (4.39), results in the dispersion relation [Kesari *et al.* (2010)]. The disc loaded circular waveguide structure which is operating in the TM mode, has applied for the high power linear accelerators while TWTs as its slow-wave RF interaction structure. By putting the ratio of disc periodicity to disc thickness as unity ($L/T = 1$), the derived dispersion relation (4.39) passes to the dispersion relation of the conventional cylindrical waveguide of disc radius.

4.3 Results and Discussion

In most practical situations, metal disc loaded coaxial waveguide finds application in the high power microwave devices (Figure 4.1). For the validity of the equivalent circuit approach, developed in our case, the dispersion characteristics of a set of the typical structure parameters with reference to the typical operating modes TM_{00} (TEM) and TM_{01} are plotted with the help of the relation (4.39). These expressions closely agree with those obtained using the dispersion relation obtained by the field analytical approach. The dispersion relation also obtained through the electromagnetic simulation (using CST Microwave Studio) and results are plotted and shown in Figures 4.2(a) and (b).

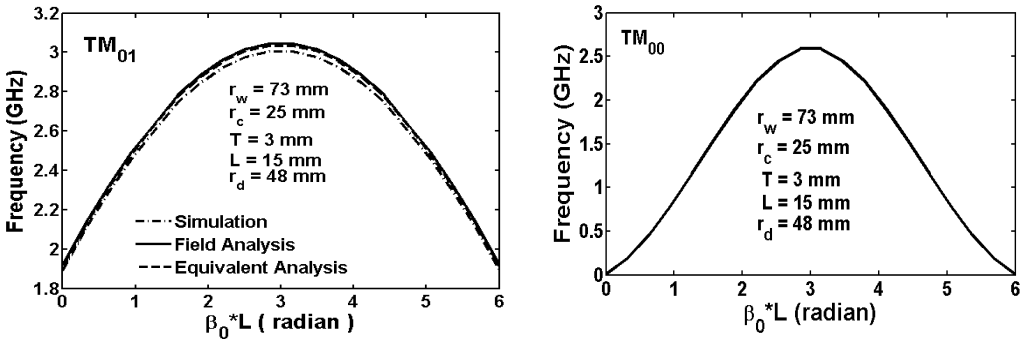

(a) (b)

Figure 4.2: Dispersion versus frequency plot for (a) TM_{01} mode, (b) TM_{00} mode of the disc-loaded coaxial cylindrical waveguide structure.

The dispersion curve for a typical disc loaded coaxial structure parameter for the TM_{01} mode while taking into account lower and higher order values of *n* and *m* and is plotted as Figure 4.3. As expected, it is found to be periodic on the scale of frequency with the periodicity of $\beta_0 L = 2\pi$ which is in agreement with the field analytical values.

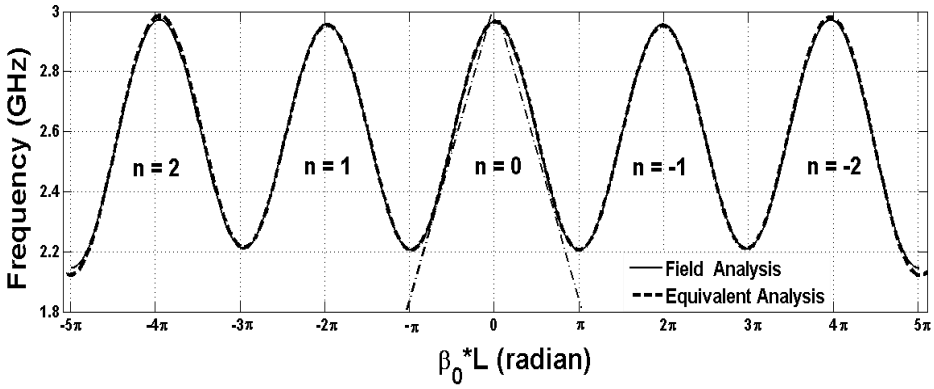

Figure 4.3: Pass and stop band characteristics of a disc loaded coaxial waveguide structure showing the effect of lower order harmonics (n= 0, ±1, ±2).

Further, it can be seen from Figure 4.3 that the slow-wave i.e. waves with $v_{ph} < c$ may exist in the periodic structure under consideration is in accordance with Floquet's theorem. It can be concluded from Figure 4.3 that the coaxial disc loaded waveguide exhibits alternate pass and stop bands with their respective cut-off frequencies for the typical structural parameters. Device operating point is obtained from the intersection

of the dispersion curve with the beam mode line which corresponds to the synchronism condition.

4.3.1 Effect of structural parameters on propagation characteristics

It is of interest to study the variation of equivalent line parameters such as series inductance per unit length and shunt capacitance per unit length with the frequency and structure dimension. From the respective expressions, it is observed that both of these line parameters depend on disc hole radius r_d and periodicity between the metal discs L. Further, the effect of the four structural parameters: disc hole radius r_d, waveguide wall radius r_w, discs periodicity L and cathode radius r_c is also numerically appreciated.

Figure 4.4(a) shows an increasing pattern of shunt capacitance which helps to understand the concentration of electric field on the beam axis that further increases the transit time factor. According to the frequency relationship, increase of the capacitance in turns lowered inductance to maintain the same resonant frequency which can be observed from Figure 4.4(b). For the typical structure parameters and chosen coaxial waveguide mode variation of the series inductance with frequency is plotted for the different disc hole radii in Figure 4.4(b). Series inductance goes down because the amount of magnetic energy stored reduced for the smaller cavity radius. It can be further observed from Figure 4.4 that the typical electromagnetic coupling exists from one cavity to another which is due to the capacitive coupling at the bottom of resonance cavities and weak mutual inductance coupling at the top.

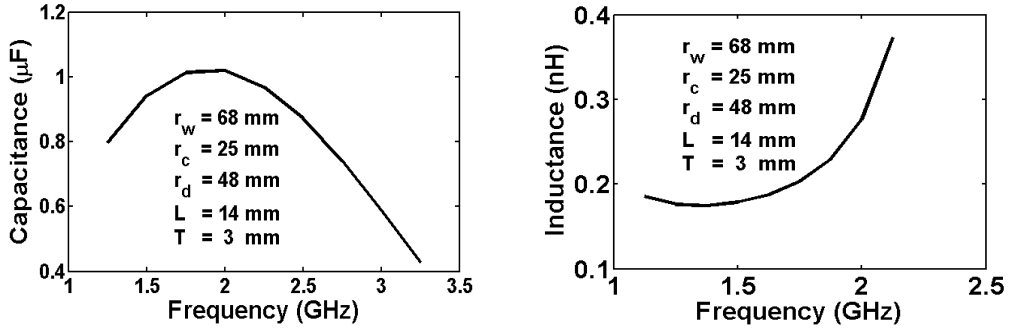

(a) (b)

Figure 4.4: Variation of **(a)** shunt capacitance and **(b)** series inductance per unit length of the equivalent transmission line of the disc loaded coaxial structure versus operating frequency.

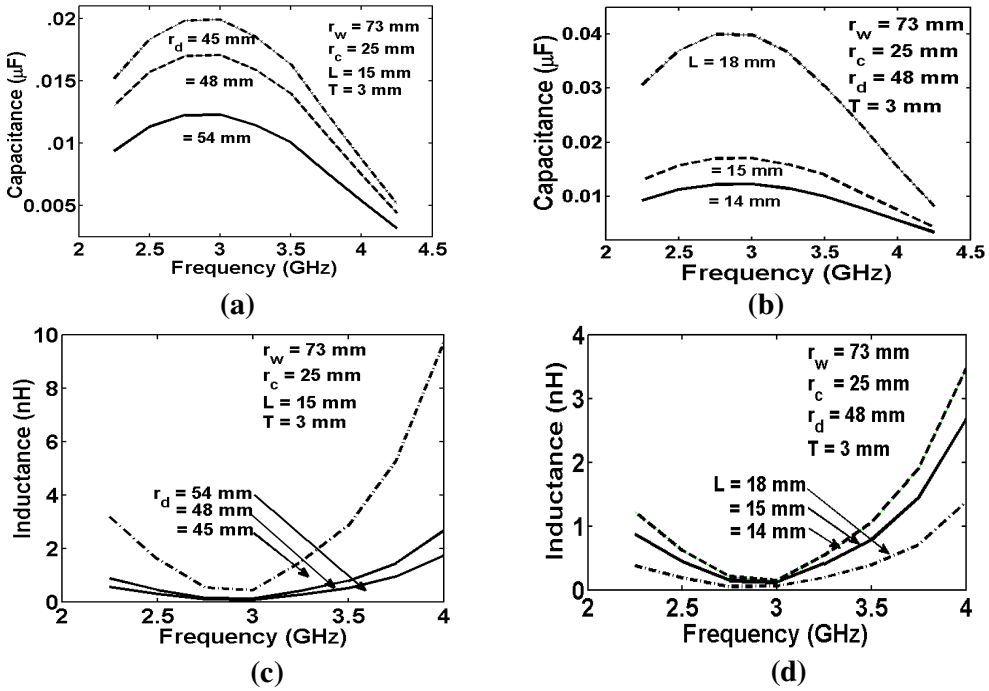

Figure 4.5: Variation of **(a)** shunt capacitance and **(b)** series inductance per unit length versus frequency plot taking the disc radius (r_d) as the parameter, **(c)** shunt capacitance and **(d)** series inductance per unit length versus frequency plot taking the disc periodicity (L) as the parameter, for a disc loaded coaxial waveguide structure.

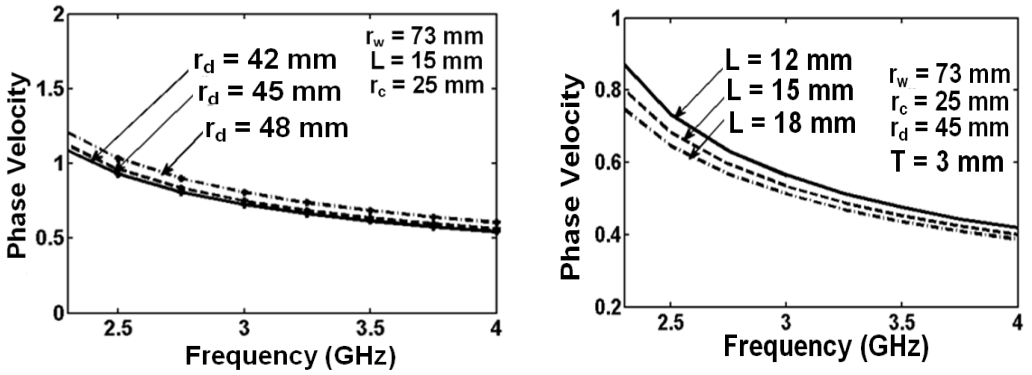

(a) (b)

Figure 4.6: Variation of phase velocity (v_p/c) versus frequency plot of a disc loaded coaxial waveguide structure with **(a)** the disc hole radius r_d and **(b)** disc periodicity L as the parameter.

Figures 4.5(a) and 4.5(b) exhibit the effect of the disc hole variation on shunt capacitance and series inductance of the equivalent line. Figures 4.5(c) and (d) show the effect of the discs periodicity on these line parameters. Effect of the waveguide radius on equivalent capacitance of the line can be observed from Figures 4.4(a) and 4.5(a). It can be concluded that this variation lead to decrease in shunt capacitance of the structure. Less variation in capacitance has been observed from Figures 4.5(a) and 4.5(c), on varying disc hole radius and periodicity. Further, it can be concluded from Figures 4.6(a) and 4.6(b) that varying disc hole radius and discs periodicity results in decrease in the phase velocity of the structure. Furthermore, the phase velocity variation with frequency reduces at the higher frequencies. Thus, disc loaded coaxial waveguide results in maintaining synchronism (that is reducing the phase velocity of RF during beam-wave interaction mechanism). Hence, it could be concluded that disc-hole radius and disc periodicity are the two important structure parameters for designing of this type of structure.

4.3.2 Effect of structural parameters on dispersion characteristics

The dispersion relation for a metal disc-loaded coaxial waveguide structure obtained by the present equivalent circuit analysis is used to study the effect of disc parameters such as disc hole radius and disc periodicity considering the effects of the finite disc thickness and higher order harmonics.

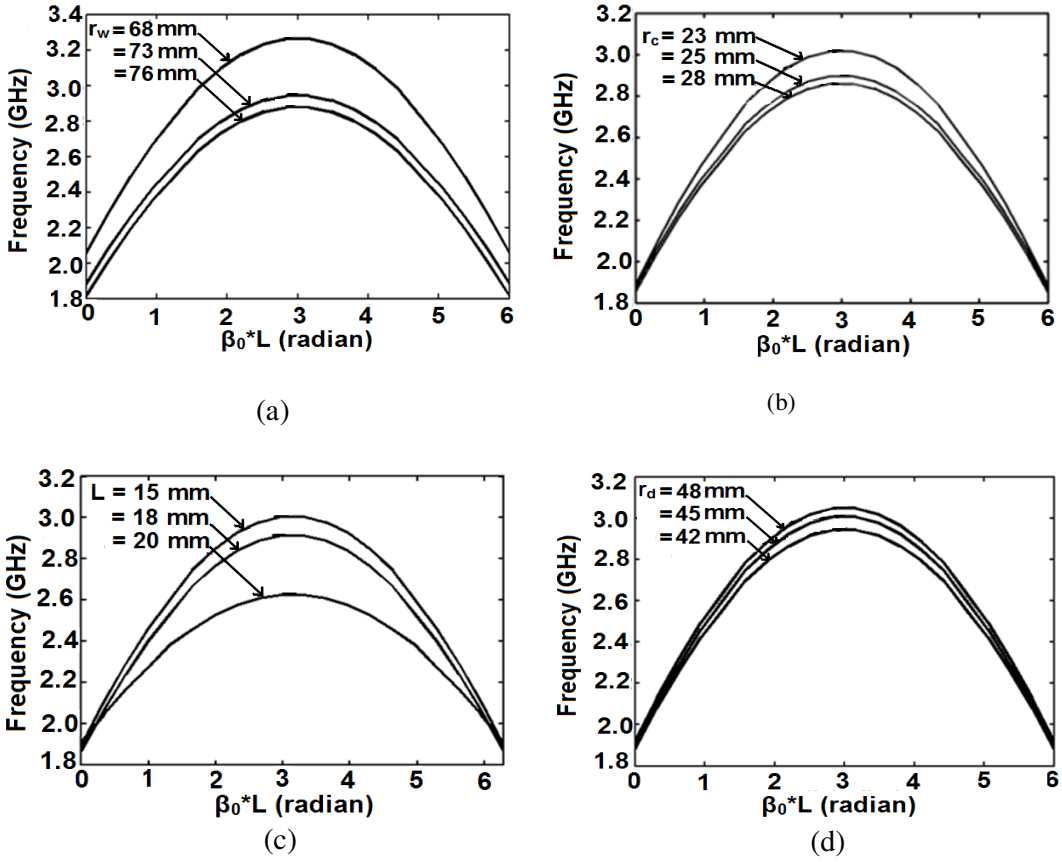

Figure 4.7: Dispersion: phase velocity ($\beta_0 L$) versus frequency plot of a metal disc loaded coaxial waveguide structure with **(a)** waveguide radius r_w, **(b)** cathode radius r_c, **(c)** disc periodicity L and **(d)** disc hole radius r_d as the parameters, for the typically selected structure parameters r_w = 73mm, r_c=25 mm, L=15 mm, r_d=48 mm, T=3mm.

Here, dispersion characteristics for a typical structure parameter are plotted for the TM_{01} mode operation while considering higher space harmonics. It is found that the

shape of the dispersion characteristics depends on the disc-hole radius and the structure periodicity which is being more sensitive to the latter. From Figure 4.7, one can get information about the device operating point and cut off frequency. Figure 4.7(a) shows that the variation in waveguide radius affects the cutoff frequency of the structure. Cutoff frequency linearly depends on eigenvalue of the particular mode and inversely proportional to waveguide radius. As expected the increase of the waveguide radius, downward shifts its cutoff frequency. Figure 4.7(b) exhibits the same pattern as observed in case of variation in waveguide radius with central conductor radii while keeping all other structure parameters same. It can also be seen from Figure 4.7(c) that with increase in periodicity device operating frequency decreases. Further, it is also observed from Figure 4.7(d) that there is less variation in operating frequency with the variation of the disc-hole radius (r_d) of the structure, however, there is reduction in the structure pass band. Thus the disc periodicity is an important parameter that affects the dispersion characteristics of the structure [Jian-Qing *et al*. (2005)].

4.4 Conclusion

An axially periodic metal disc loaded coaxial cylindrical waveguide structure is frequently used in RF systems as slow- and fast-wave RF line for the passive and active devices. The electromagnetic analysis of such structures has already been performed using the modal field analytical approach. Such analysis gives accurate result nevertheless is rather involved and yields cumbersome dispersion relation. To make the analysis simpler an alternate equivalent circuit analytical approach is adopted. In our study the actual structure is replaced by an equivalent transmission line in terms of its equivalent circuit parameters. Assuming the loss free condition

only two parameters: the series inductance and shunt capacitance per unit length of the line has been used for analysis. These two parameters are derived independently and one has to deal with only half of the total structure EM field expressions and boundary conditions at a time which makes the analysis simpler and yields relatively much simple expression. The dispersion characteristics obtained by the present equivalent circuit approach exactly passes to those expressions which were obtained through the field analysis. The computed results are also found to be in close agreement with those obtained through electromagnetic simulation. Furthermore as special cases, the derived dispersion relation can also be used for disc loaded cylindrical waveguide and for a conventional cylindrical waveguide, too. The characteristic impedance of the line which is an important parameter while considering circuit matching condition can also be obtained through the analysis. Through computational simulation analysis it is found that the control of dispersion characteristics depends on disc-hole radius and the structure periodicity which is more sensitive to the latter. The present analysis is carried out for the slow-wave case and for the TM_{0n} operating mode, though the approach is general and can be adopted for the analysis of such structures operating for fast-wave or TE_{mn} mode, also. It is hope that the present equivalent circuit analytical approach would prove handy to the RF engineers for analysis and design of metal disc-loaded periodic waveguide structures.